# REPORT DOCUMENTATION PAGE

Form Approved
OMB No. 0704-0188



| 1. AGENCY USE ONLY (Leave blank) | 2. REPORT DATE | 3. REPORT TYPE AND DATES COVERED |
|---|---|---|
| | December 26, 1994 | |

**4. TITLE AND SUBTITLE**
**Measurement of Interface Strength, Intrinsic Toughness and Their Dependence on Interfacial Segregants**

**5. FUNDING NUMBERS**

**6. AUTHOR(S)**
**Professor Vijay Gupta**

**7. PERFORMING ORGANIZATION NAME(S) AND ADDRESS(ES)**
**Thayer School of Engineering**
**Dartmouth College, Hanover,**
**New Hampshire, 03755, U.S.A.**

**8. PERFORMING ORGANIZATION REPORT NUMBER**

**9. SPONSORING/MONITORING AGENCY NAME(S) AND ADDRESS(ES)**
U.S. Army Research Office
P.O. Box 12211
Research Triangle Park, NC 27709-2211



**10. SPONSORING/MONITORING AGENCY REPORT NUMBER**

**11. SUPPLEMENTARY NOTES**
The views, opinions and/or findings contained in this report are those of the author(s) and should not be construed as an official Department of the Army position, policy, or decision, unless so designated by other documentation.

**12a. DISTRIBUTION/AVAILABILITY STATEMENT**
Approved for public release; distribution unlimited.

**12b. DISTRIBUTION CODE**

**13. ABSTRACT** *(Maximum 200 words)*

This report discusses a novel laser spallation technique for measuring the tensile strength of planar thin film interfaces. In this technique, a laser-produced compressive stress pulse in the substrate, reflecting from the coating's free surface pulls the interface in tension and leads to its failure if the tensile amplitude is high enough. The interface stress is determined by recording the coating or substrate free-surface velocities using a Doppler interferometer. Interface strengths of several metal/ceramic, ceramic-ceramic and ceramic/polymer systems are summarized from our recent efforts. In addition, two breakthroughs, the first of a novel interferometer to record velocities from rough surfaces, and the second of a technique to produce subnanosecond rise-time stress pulses with no asymptotic post-peak decay, are discussed which further allows the technique to be applied to rough thermal spray coatings and also to films as thin as 0.1 μm. This technique is used to establish a fundamental strength-structure-chemistry relationship for Nb/sapphire interfaces, with and without the interlayers of Cr and Sb. This allows the interface strengths to be controlled over a wide range, as required for realizing the strategy of deflecting impinging matrix cracks along the fiber/matrix interfaces so as to impart toughness in otherwise brittle composites. The required values of fiber/matrix interface toughness needed for crack deflection were obtained by using the method of dual singular integral equations. Finally, in a separate study, the short stress pulses are used to determine the dynamic response of laminates, and preliminary results are presented that show their potential in evaluating the damage in composites in a non-destructive mode.

| 14. SUBJECT TERMS | 15. NUMBER OF PAGES |
|---|---|
| Interface strength; laser spallation experiment; interface toughness; Doppler interferometer; metal/ceramic interfaces; interface crack deflection, composites;spall, dynamic strength, non-destructive evaluation. | 42 |
| | 16. PRICE CODE |

| 17. SECURITY CLASSIFICATION OF REPORT | 18. SECURITY CLASSIFICATION OF THIS PAGE | 19. SECURITY CLASSIFICATION OF ABSTRACT | 20. LIMITATION OF ABSTRACT |
|---|---|---|---|
| UNCLASSIFIED | UNCLASSIFIED | UNCLASSIFIED | UL |

NSN 7540-01-280-5500

Standard Form 298 (Rev 2-89)
Prescribed by ANSI Std Z39-18
298-102

# Measurement of Interface Strength, Intrinsic Toughness and Their Dependence on Interfacial Segregants



## Final Report


*Professor Vijay Gupta*


**December 26, 1994**


**U.S. ARMY RESEARCH OFFICE**

**Contract Number: DAAL03-91-G0059**



*Thayer School of Engineering*
*Dartmouth College, Hanover, NH 03755.*

# I. Table of Contents

## II. LISTINGS OF TABLES, FIGURES AND APPENDICES

### List of Tables



### List of Figures



### List of Appendices

## III. REPORT ON THE SCIENTIFIC FINDINGS

## A. INTRODUCTION: STATEMENT OF THE PROBLEM STUDIED

The mechanical properties of the interfaces between coatings and substrates have become the focal point of my research in several fields, including composite materials, tribology, thermal spray, and in the solid state device area. This is because the interfaces between dissimilar materials are sites for mechanical stress concentrations and often become the nucleus of the overall failure process. In composite materials, interfaces between fibers and their diffusion barrier coatings are of interest, while in other thin film applications, those between functional (magnetic, conducting, optical, and electrical), protective (thermal barrier, corrosion, wear resistant), and decorative coatings and their underlying substrates are important. Finally, metal/ceramic interfaces are of interest in multilayer devices and in magnetic disc and head technology. Since in most applications the mechanical properties of the interface (tensile and shear strength, toughness, etc.) often control the terminal failure process, improvement in these properties for prolonged life of the coated part is of fundamental interest. However, in ceramic and metal matrix composites, where the fiber/coating interface is used to deflect impinging cracks from the matrix, it is often desirable to impair the strength of the interface. To accomplish either of the above goals, the first step is to measure reliably the fundamental mechanical properties of the interface, and establish their relationship to the interface structure and chemistry so that the interface properties can be optimized to the desired level. Accordingly, the major thrust in this research has been to develop a laser spallation technique to measure the tensile strength of planar interfaces, and to show how this experiment measures an *intrinsic* response of the interface.

Almost all other available techniques for measuring interface strength [1] involve a nonhomogeneous stress field in the vicinity of the interface. Besides producing premature fracture elsewhere before the intended interface can be probed, significant plastic deformation accompanies the failure, which totally masks the fundamental energy or strength required to decohere the interface. In addition, such processes disallow any correlation of the *individual* processing variables used for surface or microstructural tailoring onto the mechanical response of the interface. Rather, they give a combined effect and one with no direct correlation to the fundamental attributes responsible for adhesion. One of my main contributions in this area has been to develop a laser spallation experiment which overcomes this shortcoming and provides a measure of the *actual* tensile strength of the interface by probing the local interface structure with a sharp stress pulse. As discussed later, the interface tensile strength measured by this technique is fundamentally related to the *intrinsic* toughness of the interface. The tensile strength thus obtained can be directly related to the interfacial microstructure.

## B. SUMMARY DESCRIPTION OF IMPORTANT RESULTS

### B1. Measurement of the Interface Tensile Strength by a Laser Spallation Experiment

The focus of our work was to modify a laser spallation technique I had developed at M.I.T. as a part of my doctoral thesis research. As discussed below, several significant changes have been made, which now makes the technique more versatile and convinces us of its ability to measure a fundamental mechanical response of an interface.

*B1.1. M.I.T. Version of the Technique*

The experimental approach utilizes a planar arrangement of a substrate and coating combination, as shown in Fig. 1. Details of the sample holder are given in Gupta *et al.* [2,3]. The collimated laser pulse is made to impinge on a 1-μm thick gold film that is sandwiched between the back surface of a substrate of interest and a fused quartz confining plate, transparent to the wavelength of the laser (Nd:YAG laser operated at 1.06-μm). Absorption of the laser energy in the confined gold leads to a sudden expansion of the film which, due to the axial constraints of the assembly, leads to the generation of a compressive shock wave directed toward the test coating/substrate interface. A part of the compressive pulse is transmitted into the coating as the compression pulse strikes the interface. It is the reflection from the free surface of the coating of this compressive pulse into a tension pulse that leads to the removal of the coating, given a sufficiently high amplitude. A key element of the experiment was to determine the amplitude of the interface tensile stress at the threshold laser fluence causing the interface failure.

Previously, the approach consisted of a three-part strategy. The first part was the development of a finite element computer simulation of the conversion of the laser light pulse into a pressure pulse, and of the resulting history of tensile stress which develops at the interface as the wave is reflected from the free surface of the coating. In the second part of the strategy, the pressure pulses were measured in a microelectronic, piezoelectric device in which the conditions of the computer simulation were experimentally achieved. This permitted verification and fine tuning the computer simulation. Finally, actual spallation experiments were carried out for several thin coating/substrate interfaces (e.g., C/Si and SiC/Si interfaces). The laser fluence necessary for the removal of the probed portion of the coating at the interface was recorded, and the tensile stress across the interface that accomplished this was determined from the computer program. The analysis of the post-spalled samples through detailed Auger spectroscopy showed the failure to occur at the interface in the SiC coated pyrolytic graphite and Si wafer discs. The SiC/Si interface was varied by changing the deposition conditions of the SiC coating, and accordingly, the interface strength values ranging from 3.7 to 10.5 GPa were determined. An average value of 7.2 GPa was determined for the SiC/PG interface.

*B1.2. The Dartmouth Version of the Technique*

The focus of this work was to modify the earlier version of the laser spallation technique by quantifying the interface stress with a laser Doppler interferometer. The details of the setup can be found in a series of papers [4-7]; here we provide only a brief description. The laser pulse is now made to impinge on a 0.3-μm thick aluminum film (instead of gold) that is sandwiched between the back surface of a substrate of interest and a 5-to-10 μm thick layer of solid water glass. The solid water glass layer was obtained by applying a thin layer of liquid water glass (liquid solution of sodium silicate) to the laser absorbing Al film; after several minutes' exposure in the air, water evaporates from the water glass leaving behind a layer of $SiO_2$ that is transparent to the laser wavelength.

When the stress pulse is reflected from the free surface of the coating or the substrate, the free surface experiences a transient velocity, which in turn is proportional to the transient profile of the striking stress pulse. The transient velocity was measured directly by a velocity interferometer, and also more accurately, by recording the displacement history of the coating's or substrate's free surface by a displacement interferometer, a schematic of which is shown to the right of the coating surface in Fig. 2. The peak interface tensile stress generated at each level of the laser fluence is related to the maximum compressive stress at the free surface (coating's or substrate's) through a computer simulation. In this program, a stress pulse measured at the substrate's free surface (measured in separate experiments) was made to impinge at the interface from the substrate side, and the resulting peak tensile amplitudes of the normalized stresses at the interface and the coating's free surface are determined. We then take the ratios of these calculated amplitudes and use them as transfer coefficients to convert the measured peak stress at the coating or the substrate free surface to the interface peak stress. Since the generated stress profile is similar for different laser fluence levels [7], the simple approach of using transfer coefficients is very accurate provided the coating remains elastic. The above procedure results in a plot of laser fluence vs. interface stress. This information is then used to convert the threshold laser fluence causing coating spallation to the interface strength. In cases where the substrate's free surface can be polished to a mirror-finish, we use it to characterize the laser fluence, otherwise we use the velocity measurements on the coating's free-surface for characterization of the laser fluence. Since in the new setup the stress pulse is recorded directly, the strength of interfaces involving ductile components can also be determined, as long as the wave mechanics simulation includes the elastic-plastic constitutive law for the ductile component. In view of extending this technique for future ductile systems, we have incorporated such a constitutive law in our current wave mechanics simulation [8]. However, for all materials considered so far, the measured strengths were within the Hugoint elastic limit, thereby permitting an elastic analysis to quantify the free-surface velocities.

For specular surfaces, it is possible to measure both the free surface displacement and the velocity by using the standard laser Doppler displacement and velocity interferometers which are used widely in the plate impact research. Since in our experiment, the stress pulses were sharp (rise time < 5 ns) and produced over a small area

(7 $mm^2$), recording sub-nanosecond displacement and velocity fringes posed a significant challenge. Remarkably, the displacement fringes with a 0.2 nanosecond (ns) resolution, and those obtained in the first 20 ns were recorded in a single shot mode.

The current technique is an improvement over the previous one [2], since the interface stress at the threshold laser energy is determined directly by recording the coating's or substrate's free-surface velocities using an optical interferometer. This also takes care of some of the concerns regarding the validity of a one-dimensional computer simulation for modeling the propagation of the stress pulse. In the modified technique, no stress pulse propagation model is used since the stress pulse that arrives in its final form at the coating surface is directly measured by the interferometer. For the same reason, it is no longer necessary to simulate the stress pulse generation mechanism that depends among various things upon the laser fluence, the temperature distribution in the Al film, the surrounding water glass and the constraining substrate disc, and finally, on the volumetric expansion within Al upon its melting.

Apart from the above modifications, two additional breakthroughs were recently made by our group which increased the versatility of the technique, allowing coatings with rough surfaces (e.g., thermal spray coatings) and those with thickness less than 0.1 μm to be tested. The first development was that of producing sub-nanosecond rise-times stress pulses with amplitudes in excess of 3 GPa in the substrate [9]. In contrast to earlier pulse profiles assuming an asymptotic tail at about 5% to 10% of the peak stress, these pulses show hitherto unreported, much sharper post-peak decays resulting in a zero stress at about 17 ns. Since in the laser spallation experiment, the tensile stress at the interface results after reflection of the parent compressive stress pulse from the coating surface, a sharper rise-time and a sharper post-peak decay stress pulse enhances the interface tensile stress in thin film interfaces, and films with 0.3 μm in thickness could be separated. The setup to produce such short stress pulses by using a 5-to-10 μm thick layer of solid water glass layer is discussed in Appendix I.

Another important development was that of an optical interferometer [10] which allowed us to record the velocities of rough surfaces, that otherwise destroy the geometrical coherence of the reflected beam and make the regular interferometer unusable. Now, thermal spray coatings with rough surfaces can be tested. Further, for some interface systems with very large substrate surface roughnesses, the surfaces of even very thick coatings assume the roughness of the substrate, which then disallows recording the displacement fringes from either the substrate's or coating's surfaces using the standard interferometer. The new interferometer allows us to characterize such interfaces as well. This setup is briefly discussed in Appendix II.

These techniques were used to determine the tensile strengths of a variety of interfaces of interest to the microelectronic, composites, and thermal spray industries. In all experiments, the substrate discs were either 12.7 mm or 25.4 mm in diameter and 1 mm thick. Typical test coating thicknesses ranged from 1 μm to 3 μm. The laser beam was focused onto a 3-mm diameter spot so as to keep the ratio of the stress pulse

generation area to propagation distance (thickness of the substrate) to 3, which in turn ensures a planar stress front to load the interface. The incident laser fluence was controlled by changing the energy of the laser beam while keeping the illuminated area constant.

An average value of 41 MPa was determined for the strength of interfaces between 0.1 μm thick Cu films and nitrided surfaces of Si. Additionally, the strength and failure mechanisms of interfaces between metallic coatings of Sn, Sb, Cu, Nb, Al, Cr, and substrates of pyrolytic graphite were measured in units of MPa to be 18.5, 6.0, 15.50, 41.70, 16.50 and 15.50, respectively [6]. Similarly an average value of 320 MPa for the $SnO_2$ coating/alumina interface was measured [11]. A value of 280 MPa was obtained for the Nb coating/alumina interface [12]. In addition, the strength of the Nb/alumina interface was controllably increased to 0.35 GPa by increasing the Cr interlayer thickness to 50 Å. The strength could be continuously decreased to 0.16 GPa by increasing the Sb thickness to 70Å [12]. The overall error in the laser spallation measurement stemming from the laser pulse variability, measurement of the ablated area, and recording of the fringes, etc. is estimated to be within 8%. All of the above strengths were obtained as an average of 8 to 10 measurements, and the largest variation was limited to only 10%.

The issue of how the above measurements relate to the interface properties obtained by other techniques often surfaces. As discussed earlier, the failure process in most available techniques involves a significant plastic deformation, which totally masks the fundamental energy or the strength required to decohere the interface. This disallows any correlation of the *individual* processing variables used for surface or microstructural tailoring onto the mechanical response of the interface. By contrast, since the interface is loaded at a strain rate of almost $10^7$/sec in the laser spallation experiment, all inelastic processes that usually accompany the interface decohesion process are largely avoided, and as shown in Gupta *et al.* [12], the measured strengths $\sigma_0$ can be related to the intrinsic interface fracture energies $G_{ci}$ using the concepts of universal bonding correlation, which have recently also been found to hold for metal/ceramic interfaces too as

$$\sigma^2_o = E_o G_{ci}/e^2 h, \qquad (1)$$

where $h$ is an unstressed separation distance between the planes joining at the interface and $E_o$ is the initial one-dimensional tensile straining modulus of the interface layer. This strength-toughness relationship was recently verified by us by measuring the interfacial energies independently by a new technique, which in turn, related fairly well to the measured tensile strengths from the spallation experiment.

In this technique [13], a test coating of 100 Å to 200 Å is deposited on the substrate of interest. This layer is then overlaid by a residually-stressed Nb coating (used as a loading device) and its thickness is controlled until it buckles the lower test layer from the substrate. By determining the intrinsic residual strain within the Nb layer in independent delamination experiments, the bilayer buckling morphology is quantified, and a measure of the interface fracture toughness is obtained. The key to the experiment

is to quantify the intrinsic residual strain within the Nb film by forcing it to buckle in a one-dimensional mode. This was achieved by depositing the Nb coating with a saw-tooth morphology onto a sapphire substrate by using the photolithographic techniques. By controlling the Nb thickness so as to be critical at its crest, and equal to half its thickness along its troughs, the Nb layer was forced to buckle in a one-dimensional morphology. The measurement of its buckled profile by using an atomic force microscope and its subsequent comparison with the unbuckled straight length readily provides a measure of its intrinsic strain. This technique has been successfully applied to interfaces between metallic coatings of Sb, Cr, Cu, Nb, Al, and substrates of sapphire with (0001) orientation. I believe that this technique can be quite important in characterizing interfaces, and can complement the information provided by the laser spallation experiment.

Although the spontaneous delamination technique is important in its own right, it can also act as a referee to the fundamental nature of the data provided by the laser spallation experiment. For example, the measured strength of a flaw-free Nb/(0001) sapphire interface of 1.9 GPa relates fairly well through eqn (1) to a value of 0.8 $J/m^2$ for the interface toughness obtained from the spontaneous delamination technique. The value of the interatomic separations were obtained independently through detailed high resolution transmission electron microscope studies discussed below. However, if the interface is flawed, the laser spallation experiment measures a value that reflects this change in the microstructure. The measured strength of a Nb/alumina interface (with interface flaws) of 0.28 GPa when compared with that of Nb/sapphire interface of 1.98 GPa (with no flaws as shown below) clearly indicates the potential of the technique to distinguish the effects of interfacial cracks and voids. Thus, the experiment seems to measure the *actual* strength of the interface, which then approaches the *intrinsic* strength if the interface is free of any defects.

Another issue that often surfaces is that of the effect of the in-plane residual stresses on the measured bond strength, and as discussed below, the laser spallation measurements are not affected by such stresses. The experiment measures a tensile strength in which the atoms are first pulled apart normal to the interface, causing an initial debond length, followed by its immediate instability in the form of delamination. The pre-existing in-plane residual stresses participate only in encouraging the later delamination process. However, as far as the laser spallation experiment is concerned, we are only interested in the initial debonding created when the atoms are first pulled away from each other; also referred to as the tensile strength of the interface (or the peak of the interface stress-separation curve). The in-plane residual stresses usually result in 3% to 4% strains (in-plane) and due to Poisson's effect, these will result in a similar strain in the normal direction. Such strains should have a little effect on the interface stress-separation curve, and hence on the measured tensile strength obtained by the laser spallation experiment. The above holds if the interface is free of cracks and mechanical roughness since in such cases the failure is controlled by continuum-scale processes, which in turn, can be influenced by the residual stresses.

With the basic interface characterization tool at hand, we are now ready to address the issue of *controlling* the interface mechanical properties to a *desired level*, as required in a specific tribological, composites, microelectronic or thermal spray engineering applications. A fundamental approach to engineered interfaces is to establish a one-to-one relationship of the interface structure to its mechanical properties, followed by optimizing the microstructure to maximize performance in a specific application. Despite its recognition by several investigators, development of such a relationship remains uncharacterized for interfaces. Although several theoretical and experimental efforts have successfully obtained the atomic structure and chemistry for metal/ceramic and polymer/ceramic interfaces, no measurement of the *fundamental* mechanical properties has been possible, and this has remained the primary obstacle in attempts to develop the strength-structure-chemistry relationships. Below we discuss how such a relationship can be obtained by taking a specific example of the Nb/sapphire interface, and controlling its strength through heat treatment and by providing interlayers of Cr and Sb of varying thicknesses.

## B2. Strength-Structure-Chemistry Relationship for Nb/Sapphire Interfaces

To control the interface strength through modifications of structure and chemistry, we measured the strength of Nb/sapphire interfaces, with and without interlayers (5-40Å thick) of Cr and Sb [14,15]. Spallation experiments were performed on Nb/sapphire, Nb/Cr/sapphire and Nb/Sb/sapphire interfaces in the as-deposited state, and also on samples with two different heat treatment cycles, viz. at 600°C for 24 hours and at 1200°C for 10 minutes. The structure was obtained with HRTEM for all interfaces, here shown only for Nb/Cr/sapphire (Fig. 3). All interfaces were flat and free of macroscopic defects like cracks and voids except those which were annealed at 1200°C for 10 minutes. With such an anneal cycle, both the Nb/sapphire and Nb/Cr/sapphire interfaces showed interfacial voids (Fig. 4), formed due to the migration of vacancies within Nb (due to the sputter deposition process) to the interface. In addition, the interfaces involving Cr showed the formation of the intermetallic compound $Cr_2Nb$, Fig. 5. Interestingly, the continuous layer of Cr is reduced to a uniform distribution of hemispherical-shaped compound. All coatings and interlayers were sputter-deposited using the RF-magnetron sputtering system. This system was assembled in-house under the ARO grant. Interestingly, as shown in Fig. 3, back-sputter cleaning of the sapphire surface via flow of Argon ions, prior to coating deposition, forms a 10-to-25 Å thick disordered amorphous layer. This layer was present in all deposition. This layer is re-crystallized at 1200°C, as shown in Fig. 6. The above structure and chemistry were related to interface strength. Figure 7(a) shows various interfaces in ascending order of their strength, as measured by the modified laser spallation experiment. The highest strength was recorded for Nb/Cr/sapphire sample annealed at 1200°C. The intermetallic compound $Cr_2Nb$ acts as a strength enhancer. Figure 7 (b) shows how by controlling the thickness of the Cr and Sb interlayers, the interface strength can be remarkably tailored over a wide range, indicating the latitude in control of interface strength possible through control of interface chemistry. Sb can lower the strength by 90%, and Cr can elevate it 50% over that for the clean interface.

Finally, the spalled samples were analyzed using XPS, Auger Spectroscopy and Atomic Force Microscopy to determine the locus of failure. All failures were at the interface adjacent to sapphire, except Nb/Cr/sapphire samples annealed at 1200°C, where the failure was non-planar, following the Nb/sapphire interface, and within Nb at locations where the intermetallic compound $Cr_2Nb$ was encountered. This was confirmed by an atomic force micrograph of the interface towards the sapphire which showed a uniform distribution of surface bumps (50-60 nm) corresponding to the anchored $Cr_2Nb$ locations. Thus, it acts as a strength enhancer. All interface failures adjacent to the sapphire were at the amorphous layer, suggesting an interesting strength-degrading mechanism in metal-ceramic interfaces.

We discuss now why interface tensile strength is an important fundamental property, and has been the parameter of interest to our studies. Both the interfacial shear and tensile strengths control the overall failure of the interface in composites and other applications. Even in the presence of an applied shear stress, the local failure is in the form of a tensile separation, because to cause interface decohesion, the atoms should be pulled apart normal to the interface. A pure mode-II component or a shear stress applied to the interfacial region at the *continuum scale* is transformed to a local tensile stress at the atomic scale. This usually happens due to the presence of second-phase compounds, interfacial imperfections, and lack of atomic coherence or atomically-flat interface. An exception is the ideal situation of an atomically-sharp and planar interface, where the atoms will simply shear past their neighbors to break initial bonds, followed by the formation of new interface bonds. In such limited scenarios, there should be a reduction in the *tensile strength* of the interface due to the re-formation of the new bonds. Although this has been shown for grain boundaries, it is unlikely to happen at heterogeneous interfaces occurring in tribological applications. Thus, for a given interface roughness on the atomic scale, a combination of an applied shear stress and a tensile stress on the continuum scale will lead to an effective local tensile stress; when this equals the fundamental strength (as provided by the spallation experiment), the interface will decohere.

It should be pointed out, however, that the interface failures in actual tribological, composite, and other thin film applications are governed by the total toughness of the interface which depends upon the extent of plastic and roughness-induced deformations, which in turn, depend upon the specific boundary value problem defining the actual ratio of the tensile to shear far-field stress probing the interface. In principle, this total toughness of the interface can be partitioned into a process-dependent inelastic dissipation energy, and the much smaller (usually 1% to 2% of the total energy) intrinsic toughness of the interface, which as discussed below, is related to the tensile strength of the interface provided by the laser spallation experiment. Although the intrinsic toughness is only few percent of the total energy needed for interface separation, it controls and scales directly with the latter since, if no energy is required to break the atomic bonds, the two bonded components will simply fall apart with no plastic deformation during the separation process. Thus, attempts to maximize the interface strength (or intrinsic toughness) by optimizing the interfacial microstructure should lead

directly to an increase in the total toughness required for interface separation, and a subsequent increase in the performance of the coated tribological components. Therefore, the thrust of our work has been to develop the intrinsic strength-structure-chemistry relationship at interfaces, and by using the Nb/sapphire interface work as a precursor, we have proposed [16] to develop such a fundamental relationship for few representative tribological substrate/coating systems.

### B3. Specific Applications to Composite Materials

One of our motivations for developing the laser spallation experiment was to measure and control the strength of fiber/matrix or fiber/coating interfaces to a predetermined level so as to deflect the impinging matrix cracks along the interface, which, besides leaving the fiber intact, also increases the toughness of the composite. To determine the mechanistic conditions for interface crack deflection, we have developed both a strength [17] and an energy criterion [18] for crack deflection at an interface between a fiber and a coating or between a fiber and the matrix. The analyses can account for elastic anisotropy in either medium, which is directly useful for designing composites with anisotropic sapphire and carbon fibers. Our solution is an extension the previous work of He and Hutchinson [24] for isotropic bimaterial pairs. These solutions were obtained by using the method of dual singular integral equations, which are of little interest to the composite processing community. To this end, we made a compendium of all the composite systems that were being pursued in the composites community, and provided specific results for the necessary interface toughness necessary for deflecting impinging matrix cracks along the interface. Table I from Gupta *et al.* [12] shows this contribution.

The final step in this strategy is to cast actual ceramic-matrix composites with interfaces which have strengths and toughnesses as suggested by the crack deflection solutions, which in turn, are to be obtained by using our work on the measurement and control of interface strength Since facilities to cast such composites are not available at Dartmouth, we have established contact with the researchers at the University of Cincinnati, and New Mexico Tech to pursue this research. Preliminary results of this collaboration with the University of Cincinnati have already taken the shape of a paper [19]. We aspire to sharpen this program by communicating with the researchers involved with processing of materials so as to develop materials from inside out!

It should be pointed out that a description of the laser spallation experiment and the applied mechanics calculations of the required interface toughness to achieve overall composite toughness has been included in a recent *undergraduate text* on composites by K. K. Chawla: Ceramic Matrix Composites, Chapman & Hall, 1993, pp. 192-193; 302-308.

### B4. Other Fracture Mechanics-Related Research

To understand the role of interfaces in the above toughening mechanism by interface crack deflection, it is important to determine the stress and deformation field for crack growth along interfaces between fibers and their protective coatings or those between

fiber and the matrix. Such solutions can also help address the issue of the brittle vs. ductile response of the interface. To this end, we have determined the elastic-plastic stress fields very near the tip of an interface crack on some model planar crack geometries with the ultimate aim of using them to set the overall boundary conditions for rate processes controlling the nucleation of dislocations from the crack tip, as required for studying the ductile vs. brittle response of the interface. Since most of the available solutions in the literature admit only isotropic plasticity, our analysis [20] makes provision for the anisotropic plasticity to occur in one of the media. Specifically, the solution gives the asymptotic stress fields for both growing and stationary cracks at an interface idealized as being rigid on one and single crystal on the other side. Two crack orientations with direct applications to interfaces in composite materials were considered. One orientation considered is such that the interface crack is parallel to the (001) plane with its tip along [110] and growth in the [110] direction. The second orientation considers the crack on the prism plane (0110) of an hcp crystal, with its tip along [0001] and growth in the [2110] direction. Because of the rigid substrate, families of solutions are possible. For both the stationary and growing case, solution members are found that have crack-tip stress triaxiality and normal tensile stress which are almost 40% higher than those found in homogeneous materials, which are also derived [21]. Furthermore, the effect on ductility of the orientation of the slip systems intersecting the crack tip is also discussed.

In a separate study we derived an interface strength-toughness relationship [23] by using an interatomic, interface stress separation curve based on the universal bonding correlation. This relationship has been successfully used to relate the interface tensile strengths measured by the laser spallation experiment and the interface fracture energies obtained by the new spontaneous delamination technique.

### B5. Technology Transfer

Since the interface work has the attention of many thin film companies and laboratories in the U.S., Japan, and Europe, we continue to facilitate the transfer of the laser spallation technology to various companies. With the sharp stress pulses we have successfully measured the strengths of thin film ($< 0.1$ μm) interfaces. Interfaces between $SiO_2$ and $Si_3N_4$ substrates and polyimide coatings are important in packaging applications. Over the past four months we have been working with the Digital Equipment Corporation in Massachusetts to study the above interface systems. The plan is to establish the strength-structure-chemistry relationship for the above interfaces by using different chemistries of polyimide coatings. This year I will be working with researchers at Bell Laboratories in New Jersey to adapt the spallation technique for multilayer systems. The stress pulse will be generated in the Si wafer and propagated towards the $Si/SiO_2/Al/SiO_2$ assembly. The aim is to reduce the tensile strength of the upper $SiO_2/Al$ interface to ease decohesion, by changing the chemistry of the $SiO_2$ passivation layer, which in turn will be controlled by changing the deposition conditions.

## B6. Future Research and New Directions

### *B6.1. Measurement of In-situ Fiber/Matrix Interface Strength*

The development of the laser spallation technique was motivated by the need to measure the strength of interfaces between cylindrical fibers and their coatings. However, even with the new developments at Dartmouth, it is only possible to test planar interfaces. Based on the results shown in Fig. 8, it appears that we can use the technique directly on the cylindrical fiber/matrix or coating interfaces. The figure clearly shows the separation of the individual carbon fibers from the polyimide matrix when the region shown in the figure was uniformly loaded to a stress $\sigma_0$ by the stress pulse. The challenge here is to relate the overall measured $\sigma_0$ to the local fiber/matrix interface stress by a numerical wave mechanics simulation, which is being attempted in Alexander's Ph.D. work.

### *B6.2. The Effect of Processing and Surface Variables on Adhesion*

We are using the above experimental procedures to develop a basic understanding of the various physical, chemical, and mechanical bonding mechanisms that are responsible for joining a metal to a ceramic and a polymer, and those between two ceramic components. The main goal is to understand the effects of coating microstructure (grain size and orientation), substrate roughness and orientation, interlayer of a ternary element with varying thicknesses, heat-treatment, and oxygen fugacity, on the adhesion of various two component systems discussed above. The interface systems to be studied are of technological importance, and are currently used in microelectronics, composites, paint, aircraft engines, and magnetic disc and head technologies.

### *B6.3. Measurement of Interply Tensile Strength in Laminated Composites*

Under a separate program sponsored by the Office of Naval Research, we studied the behavior of two-dimensional carbon/carbon (C/C) and carbon/polyimide (C/P) woven laminates under compression and shear loadings. We found that the local failure was due to the propagation of inter-ply cracks in both these materials. Hence, to provide the material property that sets the local failure criterion in our models, it was necessary to measure the interply tensile strength. Measurement of the transverse tensile strength is difficult by conventional test methods due to the small thickness of the manufactured laminates. We measured the interply tensile strength of C/C and C/P laminates by adapting the laser spallation technique discussed earlier. A schematic of the experimental setup used is shown in Fig. 9. Here the compressive stress pulse is produced normal to the plies, which upon reflection into a tension pulse from the sample's free surface separates the interply interface. The tensile stress causing the damage is recorded directly by measuring the transient free-surface velocity by the new interferometer (shown towards the right-bottom of Fig. 9), that is capable of obtaining the displacement fringes from the rough composite surface. The velocity profile thus obtained is converted into the stress pulse profile by using the effective elastic properties of the laminate. For these experiments, the C/C and C/P samples were cut into specimens with square cross-sections

of side 1.27 cm, and with thickness in the range 2.5 mm-3.0 mm. The sample's back surface was polished and sputter coated with a thin (10 μm thick) coating of aluminum to aid in recording of velocity fringes by the optical interferometer. Narrow square grooves corresponding to 3 to 4 laminate depths were made on the sample's front surface. The area of the squared groove was approximately equal to the laser impact area of 7 $mm^2$. The ratio of the diameter of the laser ablated area to the thickness of the substrate was maintained at 3 so as to keep 40% of the rear stressed area to be planar. Since the stress pulse is produced only on a part of the laminate surface, our preliminary experiments on ungrooved samples measured higher threshold laser energies as the failure involved rupturing of the fiber bundles along the edges of the loaded area. This problem was circumvented by using the grooved sample geometry which leads to the separation of one of the square coupons at the threshold laser energy. Tensile strength values in the range 25-30 MPa were obtained in about 20 successful spallation tests for C/C laminates, and those in the range 190-220 MPa for the C/P laminates. For both materials, the failure of the sample was characterized by the complete separation of the plies at the interply interface (Fig. 10) and at times, within the fiber bundle itself (Fig. 11). Essentially, at both deformation sites we are measuring the local fiber/matrix interface strength. When the failure is at the interply interface, the local geometry includes fibers bonded by the matrix in the two orthogonal directions (each belonging to a warp or fill bundle), whereas intrabundle fracture on the local scale is between two fibers bonded along the same direction. The values obtained by this experiment can be considered as a continuum-scale tensile strength even though the failure on the local scale envelops the failures within the matrix, and at the fiber/matrix interface (Fig. 8). This value was used as the failure condition in our models.

*B6.4. High Strain Rate Deformation of Composite Laminates*

The nanosecond pulses can be used to determine the high strain rate response of laminates, as needed to understand failure of composites under impact loading. Damage under such a loading is similar to that encountered in a steel armor plate struck by a projectile where the failure is through the formation of a material spall from its rear surface. In composites, damage also includes several interply delaminations near the rear surface and is oriented normal to the stress wave direction. Such dynamic stress waves can result from an impact of a projectile on the front surface of a composite structure, or in C/C composites, through a sudden heating of the inner surface of the composite when used in exhaust cones and heat-shielding tiles in space shuttles and rockets. Delaminations can also occur in wings and turbine blades when struck by flying birds. Thus, an understanding of their behavior under such loads is warranted. The stress pulse amplitude responsible for the onset of such a damage is taken as the effective interply strength measured above. With this as the local failure criterion, additional information on the attenuation and dispersion characteristics associated with the propagation of such pulses through the composite microstructure is needed to allow for a complete design of laminated structures subjected to a *given* impact. We have measured the dispersion characteristics of a short stress pulse as it propagates normal to the plane of the 0°/90° laminate in both the C/C and C/P materials. This short pulse can be considered as a

collection of harmonic waves of several different frequencies, mostly in the high frequency regime. As the short stress pulse interacts with the cracks, voids (only in C/C), crimps, interply interfaces, and matrix-rich pockets within the microstructure, it experiences both the shortening and broadening of its profile during its propagation. Using the novel interferometer, we have experimentally obtained the resulting stress profile in different thickness samples. Figure 12 gives the experimentally measured profiles after the initial pulse (shown with solid line) has traversed a known thickness of the C/P sample. By taking the ratios of the Fourier transforms of the incident and the net profile at a known thickness), both the real and the complex part of the wave number can be obtained. The imaginary part provides the dispersion characteristics for different frequencies (Fig. 13b for C/P and 14 for C/C) whereas the real part provides information on the frequency dependent -wave velocity ( Figs 13a). When the information given in Figs 13 is combined with the local value of the interply strength, one can design the thickness of a typical composite plate that is subjected to a *given* impact loading (i.e., with a known amplitude and frequency components). If one fixes the interply strength, then by using the information in Fig. 13 one finds how much will be the dissipation in the pulse amplitude, giving the desirable thickness directly. Since the dynamic behavior of composites is likely to become an important problem, we have already started working in this area and have obtained significant results, which are contained in Pronin *et al.* [22].

*B6.5. Non-Destructive Evaluation of Composite Laminates*

Another important area that can be addressed using the above experimental procedures is to evaluate the composite laminates for cracks and voids in a non-destructive mode. The current efforts are to relate the information in Fig. 13(b) to the crack lengths and density in the C/C laminates. The new science which is different than the classical NDE methods is in the use of nanosecond stress pulse profiles in our setup, which can see flaws much smaller than what the currently available techniques can achieve. The potential for the carbon-carbon composites (which has several pre-existing cracks) is evident when we compare its wave dispersion characteristics (Fig. 15) with that obtained for the carbon-polyimide laminates with no pre-existing cracks (Fig. 12). To make a more quantitative evaluation of the data on C/C, work is in progress, and it essentially involves doing a wave mechanics simulation where a given pulse profile is made to impinge a volume flaw, and its net profile that results after such an interaction is computed. This is to be followed by putting a collection of cracks in the material volume. The results of the simulation will be compared directly with the interferometric measurements of the net profile as it strikes the sample's free surface after completing its crack-interacted journey. Such simulations are on-going as a part of the Ph.D. thesis work of my student Alexander Pronin.

An even more powerful application is to adapt the above developments for non-destructive testing for small flaws in brittle polycrystalline materials-a process of importance in quality control. Because of the ultra short rise-time, small flaws will interact geometrically with the pulse, and the resulting profile of the pulse that emerges at the sample's free-surface will be recorded by the Doppler interferometer. By comparing

the profile of the final pulse with the base signal from a flaw-free material (or that of an acceptable quality), it should become possible to evaluate the quality of the final product or a part. Since both the pulse generation and recording are to be achieved by non-contact optical techniques, it becomes possible to assess the quality of the part during its processing history, including high temperature steps. The effectiveness of this technique has already been shown in determining the quality of the metal-to-metal bond in a non-destructive manner while working with the manufacturing division of the Ford Motor Company this past Summer. We can determine the nature (cured vs. uncured), thickness and presence of interfacial delaminations at the epoxy/metal interface. This specific study has implications for manufacturing future light weight cars where epoxy joints are expected to replace the current welds.

## B7. ACKNOWLEDGMENTS

We are greatly indebted to Dr. Edward Chen of the Army Research Office in North Carolina for his encouragement that resulted in a fruitful submission of this proposal. Subsequently, we enjoyed the freedom, support and encouragement of Dr. Wilbur Simmons of the same agency, who during the course of this research made useful suggestions. Finally, we acknowledge some useful discussions with Dr. Robert Reeber which helped us to address some relevant applications.

## C. LIST OF PUBLICATIONS

### Journal Publications


1. "The effect of microstructure and chemistry on the tensile strength of Nb/Sapphire interfaces, with and without the interlayers of Cr and Sb," J. Yuan and V. Gupta, Acta Metallurgica et Materialia, in press.

2. "Structure and chemistry of Nb/Sapphire interfaces, with and without the interlayers of Sb and Cr," J. Yuan, V. Gupta and M. Kim, Acta Metallurgica et Materialia, in press

3. "Recent developments in the laser spallation technique to measure the interface strength and its relationship to interface toughness with applications to metal/ceramic, ceramic/ceramic and ceramic/polymer interfaces," V. Gupta, J. Yuan and A. Pronin, Journal of Adhesion Science and Technology, **8**, 6 (1994) 713-747.

4. "Energy criterion for crack deflection at an interface between two orthotropic media," D. Martinez and V. Gupta, Journal of the Mechanics and Physics of Solids, **42**, 8 (1994) 1247-1271.

5. "Measurement of interface strength by the modified laser spallation technique. Part I: Experimental technique and modeling the spallation process," J. Yuan and V. Gupta, Journal of Applied Physics, **74**, 4 (1993), 2388-2396.

6. "Measurement of interface strength by the modified laser spallation technique. Part II: Applications to metal-ceramic interfaces," V. Gupta, J. Yuan and A. Pronin, Journal of Applied Physics, **74**, 4 (1993), 2397-2404.

7. "Measurement of interface strength by the modified laser spallation technique. Part III: Experimental optimization of the stress pulse," J. Yuan, V. Gupta and A. Pronin, Journal of Applied Physics, **74**, 4 (1993), 2405-2410.

8. "Calculation, measurement and control of interface strength in composites," V. Gupta, J. Yuan and D. Martinez, Journal of the American Ceramics Society, **76** (1993) 305-315.

9. "Near-tip fields for a crack along an interface between an elastic-ideally plastic crystal and a rigid substrate," V. Gupta, Journal of the Mechanics and Physics of Solids, **41**, 6 (1993) 1035-1066.

10. "Nanosecond rise time laser produced stress pulses with no asymptotic decay," V. Gupta, J. Yuan, and A. Pronin, Review of Scientific Instruments, **64**, 6 (1993) 1611-1613.

11. "Measurement of the $SnO_2/Al_2O_3$ interface strength by a laser spallation technique," V. Gupta, J. Yuan, A. Pronin and K.K. Chawla, R.U. Vaidya, Scripta Metallurgica et Materialia, **28** (1993) 1371-1376.

12. "Interferometry on diffuse surfaces in high-velocity measurements," A Pronin and V. Gupta, Review of Scientific Instruments, **64**, 8 (1993) 2233-2236.

13. "Tensile crack-tip fields in elastic-ideally plastic hexagonal crystals and layered materials," V. Gupta, Acta Metallurgica et Materialia, **41**, 11 (1993), 3223-3236.

14. "Mechanisms and quantification of spalling failures in laminated composites under shock loading," A. Pronin, K. Anand and V. Gupta, submitted to the J. Composite Materials, 1994.

15. "Effect of interfacial shear strength on crack-fiber interaction behavior in ceramic-matrix composites," S. Kumaria, R.N. Singh and V. Gupta, submitted to J. American Ceramics Society, 1994.

**Special Invited Reviews**

16. "An evaluation of the interface tensile strength-toughness relationship," V. Gupta, MRS Bulletin **XVI-4** (1991) 39-45.

17. "Designing interfaces in inorganic matrix composites," J.A. Cornie, A.S. Argon and V. Gupta, MRS Bulletin (INVITED), **XVI-4** (1991) 32-38.

## BOOK CHAPTERS

1. "Recent developments in the laser spallation technique to measure the interface strength with applications to metal/ceramic, ceramic/ceramic and ceramic/polymer interfaces," V. Gupta, J. Yuan and A. Pronin, to appear in K. L. Mittal, ed., Adhesion measurements of films and coatings, Plenum Press, New York, 1994.

2. A description of the laser spallation technique and the calculations of interface toughness in composites can be found in an undergraduate text book by K. K. Chawla: Ceramic Matrix Composites, Chapman & Hall, 1993, pp. 192-193; 302-308.

## REVIEWED CONFERENCE PROCEEDING PAPERS

1. "The effect of processing and surface variables on the metal/ceramic adhesion and its role in tailoring interfaces in composites and tribology," V. Gupta and J. Yuan, in the Proc. of High Performance Composites held at the TMS Fall Meeting in Rosemont, Illinois (1994), October 2-6, pp. 193.

2. "Characterization of thin film interfaces and spalling damage in composite laminates using nanosecond rise-time stress pulses," V. Gupta, A. Pronin, K. Anand and J. Yuan, to appear in the Proc. of the ASME Symposium on Wave Propagation and Emerging Technologies to be held at the Winter Annual Meeting in Chicago (1994), November 6-11.

3. "Fracture mechanisms and effect of interfacial segregants on metal/ceramic interfaces," V. Gupta, J. Yuan and M. Kim, Proc. of the 3rd International Conference on Advanced Materials held in Tokyo (1993), September 1-4, in press.

4. "Experimental strategy to produce nanosecond rise-time stress pulses with no post-peak asymptotic tail," V. Gupta, A. Pronin and J. Yuan, Proc. of the 3rd International Conference on Advanced Materials held in Tokyo (1993), September 1-4, in press.

5. "Measurement of cleavage strength in freshwater ice crystals by a laser spallation technique," V. Gupta and T. Xuefeng, Proc. of the 12 International Offshore Mechanics and Arctic Engineering Conference IV held in Glasgow (1993), June 20-24, p. 35.

6. "Nanosecond rise-time stress pulses for materials characterization," V. Gupta, J. Yuan and A. Pronin, Proc. of the AMD Symposium on Experimental Techniques in the Dynamics of Deformable Solids, (1993), AMD-Vol. 163, ASME, New York, p. 199.

7. "Measurement of the transverse tensile strength of carbon-carbon composites using a laser spallation experiment," K. Anand, A. Pronin and V. Gupta Proc. of the 21st Biennial Conference on Carbon, Buffalo, N.Y. (1993), June 13-18, p. 60.

8. "Measurement and control of interface strength," J. Yuan and V. Gupta, Proc. of the International Conference on Laser Applications, F. J. Duarte and D. G. Harris eds., Society of Optical and Quantum Electronics McLean, Virginia (1992), p. 851.

9. "Calculation, measurement and control of interface strength for achieving toughness in composites," V. Gupta, J. Yuan, D. Martinez and J. Deacutis, Proc. of the AIME/TMS-sponsored symposium: Development in Ceramic and Metal Matrix Composites, K. Upadhya, ed., TMS Annual Meeting, San Diego (1992), March 1-5, p. 171.

10. "Measurement of interface strength by laser spallation experiment," V. Gupta and J. Yuan Proc. of the 3rd Symposium on Metallized Plastics, K.L. Mittal and J.R. Susko eds., Phoenix, Arizona (1991), October 13-18, p. 331.

## D. LIST OF PARTICIPATING SCIENTIFIC PERSONNEL

Professor Vijay Gupta: Principal Investigator
Dr. Jun Yuan: Finished Ph.D. in September 1993.
Mr. Alexander Pronin: Final year Ph.D. Student
Mr. Jianxin Wu: 2nd year Ph.D. Student
Ms. Doris Martinez: MS 1991. She was partially supported by this grant.
Mr. Lin Tang: Supported full time for two terms before he decided to accept a job offer.
Mr. Jim Deacutis, Manager for Solid State Laboratory. The project covered 5% of his salary in the first year. He helped us with the construction of the sputter system.

**Dissertations Supervised**

*Finished*

Jun Yuan (1993), " Measurement of interface strength, interface fracture mechanisms and their relationship to interface microstructure and chemistry." For this work Jun was awarded the *Charles F. and Ruth D. Goodrich Prize for outstanding thesis work.*

*Doctoral Thesis-in progress*

2. Alexander Pronin (expected 1995),"Application of laser-produced stress pulses for materials characterization: measurement of interface fracture toughness and non-destructive testing of flaws in composites."
3. Jinaxin Wu (expected 1998), "The effect of processing and surface variables on metal-ceramic adhesion."

*Masters Thesis-in progress*

4. Victor Almgren (expected June 1996), "Strength-structure-chemistry relationship for $Al/SiO_2$ interface with applications to microelectronic multi-layer devices."

*Finished*

5. Doris Martinez (1991)," Energy criterion for crack deflection at an anisotropic interface." For this work Doris was awarded the *Charles F. and Ruth D. Goodrich Prize for outstanding thesis work.*

## IV. REPORT OF INVENTIONS

*Patent Disclosures (all disclosed on October 10, 1992)*

1. Measurement of thin film interface strength by using a laser spallation technique, V. Gupta.
2. Interferometry on diffuse surfaces in high velocity measurements, V. Gupta and A. Pronin.
3. Nanosecond rise-time laser-produced stress pulses with no asymptotic decay, V. Gupta, J.Yuan.

A patent application is pending at the United States Patent Office with Serial Number 08-026,682, covering all of the above three inventions.

## V. BIBLIOGRAPHY


1. Mittal, K. L., J. Adhesion Science and Technology, **1** (1987), 247.

2. "Measurement of interface strength by laser spallation experiment," V. Gupta, A. S. Argon, D.M. Parks and J.A. Cornie, Journal of the Mechanics and Physics of Solids, **40**, 1 (1992) 141-180.

3. "Measurement of interface strength by laser pulse produced spallation," V. Gupta, A.S. Argon, J.A. Cornie and D.M. Parks, Materials Science and Engineering, **A126** (1990) 105-117.

4. "Recent developments in the laser spallation technique to measure the interface strength and its relationship to interface toughness with applications to metal/ceramic, ceramic/ceramic and ceramic/polymer interfaces," V. Gupta, J. Yuan and A. Pronin, Journal of Adhesion Science and Technology, **8**, 6 (1994) 713-747.

5. "Measurement of interface strength by the modified laser spallation technique. Part I: Experimental technique and modeling the spallation process," J. Yuan and V. Gupta, Journal of Applied Physics, **74**, 4 (1993), 2388-2396.

6. "Measurement of interface strength by the modified laser spallation technique. Part II: Applications to metal-ceramic interfaces," V. Gupta, J. Yuan and A. Pronin, Journal of Applied Physics, **74**, 4 (1993), 2397-2404.

7. "Measurement of interface strength by the modified laser spallation technique. Part III: Experimental optimization of the stress pulse," J. Yuan, V. Gupta and A. Pronin, Journal of Applied Physics, **74**, 4 (1993), 2405-2410.

8. "Measurement of interface strength, interface fracture mechanisms, and their dependence on microstructure and chemistry," Ph.D. Thesis, Thayer School of Engineering, Dartmouth College, Hanover, NH 03733, U.S.A., September 1993.

9. "Nanosecond rise time laser produced stress pulses with no asymptotic decay," V. Gupta, J. Yuan, and A. Pronin, Review of Scientific Instruments, **64**, 6 (1993) 1611-1613.

10. "Interferometry on diffuse surfaces in high-velocity measurements," A Pronin and V. Gupta, Review of Scientific Instruments, **64**, 8 (1993) 2233-2236.

11. "Measurement of the $SnO_2/Al_2O_3$ interface strength by a laser spallation technique," V. Gupta, J. Yuan, A. Pronin and K.K. Chawla, R.U. Vaidya, Scripta Metallurgica et Materialia, **28** (1993) 1371-1376.

12. "Calculation, measurement and control of interface strength in composites," V. Gupta, J. Yuan and D. Martinez, Journal of the American Ceramics Society, **76** (1993) 305-315.

13. "A new technique to measure the toughness of thin film interfaces," V. Gupta and A. Pronin, submitted to the Journal of American Ceramic Society, 1994.

14. "Structure and chemistry of Nb/Sapphire interfaces, with and without the interlayers of Sb and Cr," J. Yuan, V. Gupta and M. Kim, Acta Metallurgica et Materialia, in press

15. "The effect of microstructure and chemistry on the tensile strength of Nb/Sapphire interfaces, with and without the interlayers of Cr and Sb," J. Yuan and V. Gupta, Acta Metallurgica et Materialia, in press.

17. "Crack deflection at an interface between two orthotropic material," V. Gupta, Z. Suo and A.S. Argon, Journal of Applied Mechanics, **59**, 2 (1992) S79-S87.

18. "Energy criterion for crack deflection at an interface between two orthotropic media," D. Martinez and V. Gupta, Journal of the Mechanics and Physics of Solids, **42**, 8 (1994) 1247-1271.

19. "Effect of interfacial shear strength on crack-fiber interaction behavior in ceramic-matrix composites," S. Kumaria, R.N. Singh and V. Gupta, submitted to J. American Ceramics Society, 1994.

20. "Near-tip fields for a crack along an interface between an elastic-ideally plastic crystal and a rigid substrate," V. Gupta, Journal of the Mechanics and Physics of Solids, **41**, 6 (1993) 1035-1066.

21. "Tensile crack-tip fields in elastic-ideally plastic hexagonal crystals and layered materials," V. Gupta, Acta Metallurgica et Materialia, **41**, 11 (1993), 3223-3236.

22. "Mechanisms and quantification of spalling failures in laminated composites under shock loading," A. Pronin, K. Anand and V. Gupta, submitted to the J. Composite Materials, 1994.

23. "An evaluation of the interface tensile strength-toughness relationship," V. Gupta, MRS Bulletin **XVI-4** (1991) 39-45.

24. M. Y. He and J. W. Hutchinson, International Journal of Solids and Structures, **25** (1989), 1053.

## VI. APPENDICES

### APPENDIX I. Nanosecond Rise-Time Stress Pulses With No Asymptotic Decay

In this section, we discuss the mechanics of generating transient stress pulses with no asymptotic post-peak decay, which was used in the spallation setup. Apart from demonstrating a short rise time of 1.14 ns, and an amplitude in excess of 3 GPa, the pulse shows a remarkably sharp, post-peak decay resulting in zero stress at about 17 ns. This observation contrasts with all other reported cases of laser-produced stress pulses, which show a gradual post-peak decay resulting in a long tail, assuming an asymptotic value at about 5% to 15% of the peak amplitude. The tail results from the long penetration depth of the thermal pulse in the substrate. The use of a confining medium with higher thermal diffusivity than that of air helps decrease the penetration depth by providing an energy sink away from the direction of the substrate. Therefore, when air is used as a constraining medium for the laser-absorbing film, a long gradual tail reaching an asymptotic value of about 10% of the peak amplitude are observed at 100 ns. Using the M.I.T. version, where a 1.0 μm-thick laser-absorbing gold film was sandwiched between a piezoelectric quartz substrate and a fused quartz plate, the stress pulses obtained showed a sharper decay resulting in an asymptotic value of 15% of the peak stress at about 45 ns.

The novel setup includes producing stress pulses by using a 0.5-μm thick Al laser-absorbing film sandwiched between a 5-μm thick layer of solid water glass, and an Si substrate (used here as an example). Figure 16 shows the stress pulse profile obtained for a laser fluence of $8.67 \times 10^4$ J/m$^2$, measured at the YAG source. Apart from an amplitude increase, and a pulse risetime of 1.14 ns, this profile displays a sharper post-peak decay with the stress finally decaying to zero in 16 ns. Interestingly, the layer of solid water glass spalls off from the Si surface along with the 0.5-μm thick Al film during the microexplosion of the laser absorbing Al film.

Although a quantitative proof of the mechanism leading to such a stress profile is not attempted, a phenomenological model provides a possible mechanism. As shown by Gupta, *et al.* [2], in the laser spallation setup, one compressive pulse is produced in each the substrate and the constraining medium. It is the reflection of the compressive pulse into a tension pulse from the free surface of the solid water glass that leads to the removal of the Al film from the Si/Al interface. For a 5-μm thick layer of solid water glass and an Al film of 0.5 μm thickness, the tension pulse reaches the Al/Si interface in about 1.27 ns (assuming a longitudinal wave velocity of 8380 m/sec in $SiO_2$ and 6400 m/sec in Al). Since the laser heating pulse is 3 ns long, such a spallation process within 1.27 ns removes the heat source, resulting in the absence of a thermal tail in the generated stress pulse. Using the computer simulation developed in Gupta, *et al.* [2], the spatial temperature distribution within the first 1.27 ns was determined in the vicinity of the Al/$SiO_2$, and of the Al/Si interface. The maximum temperature at the Al/Si interface was obtained to be only 700 K, which decays to the ambient temperature within 0.5 μm of the Si substrate. Although such a temperature gradient and amplitude remain within the Si

upon the removal of the heat source entrapped within the Al film, these are insufficient to produce any comparable stresses. Therefore, the decay tail of the stress pulse shown in Figure 52 is a mechanical tail produced by the sudden impact of the Si substrate in the first 1.27 ns! In other words, the Si surface sees only a transient pressure loading in the first 1.27 ns, resulting from a pressure pulse in the Al film, produced through the laser-Al interaction and transmitted through the Al/Si interface. Figure 17 shows the stress history at the Al/Si interface in the first 1.4 ns as obtained from the simulation presented in Gupta, *et al.* [2]. Remarkably, the first sizable tension at the Al/Si interface occurs at 1.27ns. The chopped stress pulse now acts as a new boundary condition for the Si surface.

## APPENDIX II. Optical Interferometer For Non-Specular Surfaces

To record velocities of rough surfaces, a new interferometer was developed. The schematic of the interferometer is shown in Fig. 9. The beam from a frequency-stabilized He-Ne laser is brought to focus on the specimen surface by a convex lens. Light reflected from the diffuse surface is collected by the same lens and directed to a telescope, which condenses and collimates the beam. Next, a beam splitter directs the light to the two legs of the interferometer, and the returning beams are recombined at the photodiode to produce the interference fringes, which then are recorded on a Tektronix digitizer with a single-shot rise time of 5 ps. The key point of this optical setup is the second leg of the interferometer, which consists of two lenses (with focal length ( f ) equal to 50 cm each) and one mirror. Such a system of two lenses, which are separated by the sum of their focal lengths, images the mirror M2 onto the apparent position $M^*$ at exactly the same distance as the mirror M from the photodiode. For this arrangement, the actual difference in path lengths of the two optical legs of the interferometer is equal to 8f/c, which is about 13.3 ns in our case. The apparent mirror $M^*$ allows interference to occur from a geometrically incoherent light, while the necessary optical delay length needed to obtain velocity-related fringes is provided by the actual path length achieved by the position of the real mirror M.

Table I. Energy Criterion for Interface Crack Deflection for Various Metallic, Ceramic, Intermetallic, and Polymer Matrix Composites

| Medium 1, fiber | Medium 2 | | $\alpha$ | $\beta$ | $G_{ss}/G_p$ | $G_{ss}/G_p$ | $\frac{G_{ss}/G_{ss} < \phi}{\phi}$ | $\tan^{-1}(K_{II}/K_I)$ (degree) |
|---|---|---|---|---|---|---|---|---|
| | Matrix | Coating | | | | | | |
| | | | Metallic matrix composites | | | | | |
| Pitch-55 carbon | | HBE SiC | −0.6206 | −0.2113 | 0.012 | 0.011 | 0.012 | −21.72 |
| Pitch-55 carbon | | LBE SiC | 0.6292 | 0.2177 | 0.1286 | 0.1389 | 0.1389 | −9.81 |
| Pitch-55 carbon | | C (diamond) | 0.4216 | 0.0885 | 0.0952 | 0.1080 | 0.1080 | −15.22 |
| Pitch-55 carbon | Al | | 0.00964 | −0.0370 | 0.0487 | 0.0563 | 0.0563 | −7.98 |
| $\alpha$-$Al_2O_3$ | SiC | | −0.4482 | −0.2506 | 0.2056 | 0.2033 | 0.2056 | −64.09 |
| SiC | Al | | 0.7344 | 0.2372 | 0.7383 | 0.7553 | 0.7553 | −22.03 |
| Pitch-55 carbon | Mg | | 0.2226 | 0.0389 | 0.0688 | 0.0798 | 0.0798 | −7.79 |
| $\alpha$-$Al_2O_3$ | Al | | 0.4286 | 0.0963 | 0.3972 | 0.4139 | 0.4139 | −27.30 |
| SiC | Ni | | 0.3565 | 0.1090 | 0.3563 | 0.3727 | 0.3727 | −28.82 |
| | | | Intermetallic matrix composites | | | | | |
| SiC | TiAl | | 0.4436 | 0.1560 | 0.3961 | 0.4135 | 0.4135 | −27.04 |
| Nicalon | $Ti_3Al$ | | 0.1082 | 0.0190 | 0.2764 | 0.2859 | 0.2859 | −35.26 |
| SiC | $Ti_3Al$ | | 0.5028 | 0.1682 | 0.4374 | 0.4550 | 0.4550 | −25.91 |
| $B_4C$ | $Ni_3Al$ | | 0.4205 | 0.1362 | 0.3871 | 0.4040 | 0.4040 | −27.53 |
| $TiB_2$ | $Ni_3Al$ | | 0.4368 | 0.1565 | 0.3935 | 0.4109 | 0.4109 | −27.19 |
| SiC | $Ni_3Al$ | | 0.3850 | 0.1229 | 0.3692 | 0.3859 | 0.3859 | −28.27 |
| TiC | $Ni_3Al$ | | 0.3908 | 0.1220 | 0.3724 | 0.3892 | 0.3892 | −28.15 |
| $Al_2O_3$ sapphire | $Ni_3Al$ | | 0.4220 | 0.1207 | 0.5795 | 0.3911 | 0.5795 | −16.09 |
| Nicalon | $Ni_3Al$ | | −0.0385 | −0.0370 | 0.2006 | 0.2606 | 0.2606 | −44.01 |
| | | | Ceramic matrix composites | | | | | |
| $\alpha$-$Al_2O_3$ | | $SnO_2$ | −0.2096 | −0.0907 | 0.2369 | 0.2281 | 0.2369 | −51.79 |
| $\alpha$-$Al_2O_3$ | | C (amorphous) | 0.7242 | 0.2111 | 0.7276 | 0.7452 | 0.7452 | −22.33 |
| $\alpha$-$Al_2O_3$ | LAS glass | | 0.2658 | 0.0380 | 0.3223 | 0.3357 | 0.3357 | −30.75 |
| $Al_2O_3$ sapphire | | Pt | 0.4863 | 0.1098 | 0.4174 | 0.4343 | 0.4343 | −16.08 |
| $Al_2O_3$ sapphire | | Mo | 0.2049 | 0.0330 | 0.2907 | 0.3024 | 0.3024 | −16.08 |
| SiC | | $SnO_2$ | 0.1294 | 0.0115 | 0.2815 | 0.2913 | 0.2913 | −34.55 |
| SiC | LAS glass | | 0.6367 | 0.2375 | 0.5544 | 0.5714 | 0.5714 | −23.35 |
| SiC | Soda glass | | 0.7641 | 0.2610 | 0.8061 | 0.8226 | 0.8226 | −21.42 |
| $Al_2O_3$ sapphire | | Ni | 0.3949 | 0.1065 | 0.3614 | 0.3776 | 0.3776 | −16.07 |
| $Al_2O_3$ sapphire | | Nb | 0.5291 | 0.1409 | 0.4460 | 0.4633 | 0.4633 | −16.19 |
| SiC | | Pt | 0.4519 | 0.1120 | 0.4104 | 0.4274 | 0.4274 | −26.85 |
| SiC | | Nb | 0.4966 | 0.1425 | 0.4380 | 0.4555 | 0.4555 | −26.05 |
| SiC | | Mo | 0.1623 | 0.0378 | 0.2895 | 0.3010 | 0.3010 | −33.68 |
| Nicalon | SiC (bulk) | | −0.4192 | −0.1666 | 0.2440 | 0.2173 | 0.2440 | −62.17 |
| Pitch-55 carbon | SiC (bulk) | | −0.7310 | −0.2456 | 0.3226 | 0.2649 | 0.3226 | −49.68 |
| SiC | $Si_3N_4$ | | 0.1838 | 0.0438 | 0.2954 | 0.3076 | 0.3076 | −33.08 |
| SiC | Zirconia | | 0.0263 | −0.0152 | 0.2603 | 0.2659 | 0.2659 | −37.84 |
| SiC | $Al_2O_3$ | | 0.0553 | 0.0127 | 0.2656 | 0.2733 | 0.2733 | −37.00 |
| $Al_2O_3$ sapphire | LAS glass | | 0.6622 | 0.2133 | 0.5833 | 0.6004 | 0.6004 | −17.77 |
| Nicalon | LAS glass | | 0.2987 | 0.0870 | 0.3327 | 0.3473 | 0.3473 | −30.18 |
| Nicalon | $Si_3N_4$ | | −0.2529 | −0.1199 | 0.2350 | 0.2220 | 0.2350 | −53.74 |
| | | | Polymer matrix composites | | | | | |
| Pitch-55 carbon | Epoxy | | 0.9065 | 0.2792 | 0.4210 | 0.4303 | 0.4303 | −15.23 |
| S-glass | Epoxy | | 0.9237 | 0.2991 | 2.2500 | 2.2700 | 2.2700 | −19.19 |
| Kevlar | Epoxy | | 0.9462 | 0.3068 | 3.1350 | 3.1585 | 3.1585 | −18.25 |
| E-glass | Epoxy | | 0.9091 | 0.2942 | 1.9125 | 1.9315 | 1.9315 | −19.41 |
| | | | Fiber-reinforced concrete | | | | | |
| Mild steel | Concrete | | 0.9052 | 0.3877 | 1.6180 | 1.6305 | 1.6305 | −12.00 |

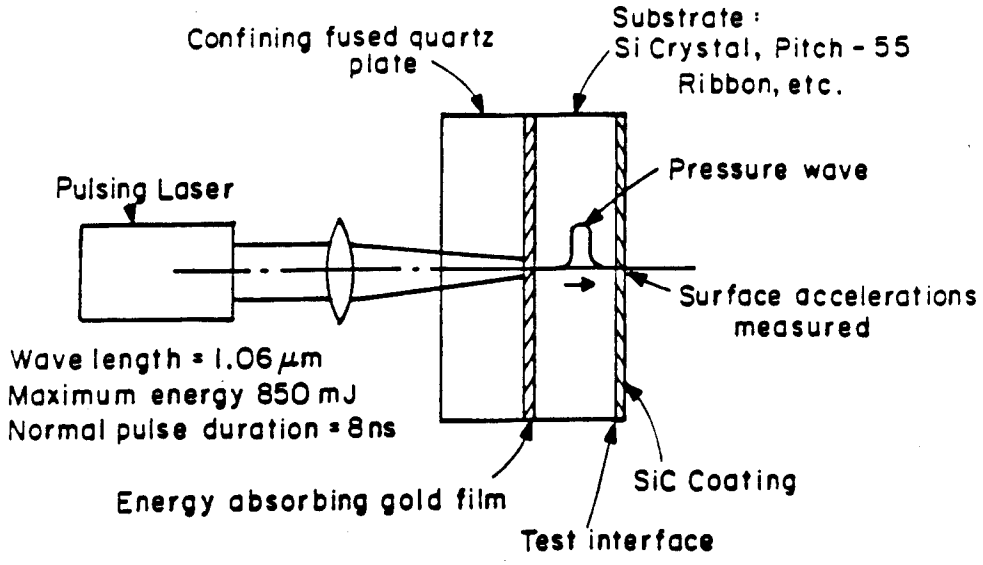


Figure 1. Schematic view of the laser spallation experiment.

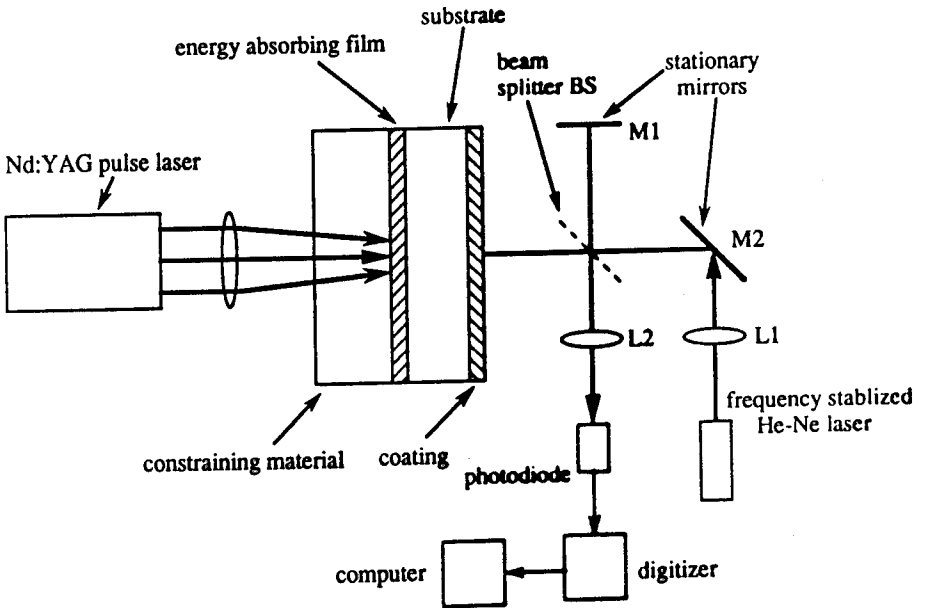


Figure 2. Schematic of the laser Doppler displacement interferometer along with the laser spallation setup.


Figure 3. High resolution transmission electron micrograph of the Nb/Cr/sapphire interface. The amorphous layer (A) formed due to the back-sputter Argon is about 25 A thick.


Figure 4. Interface voids formed at the Nb/sapphire interface after a 1200°C anneal.


Figure 5. HRTEM of Nb/Cr/sapphire interface annealed at 1200°C for 10 min. The continuous interlayer of Cr is reduced to a uniform distribution of the intermetallic compound $Cr_2Nb$ (A) at the interface between Nb (B) and sapphire.

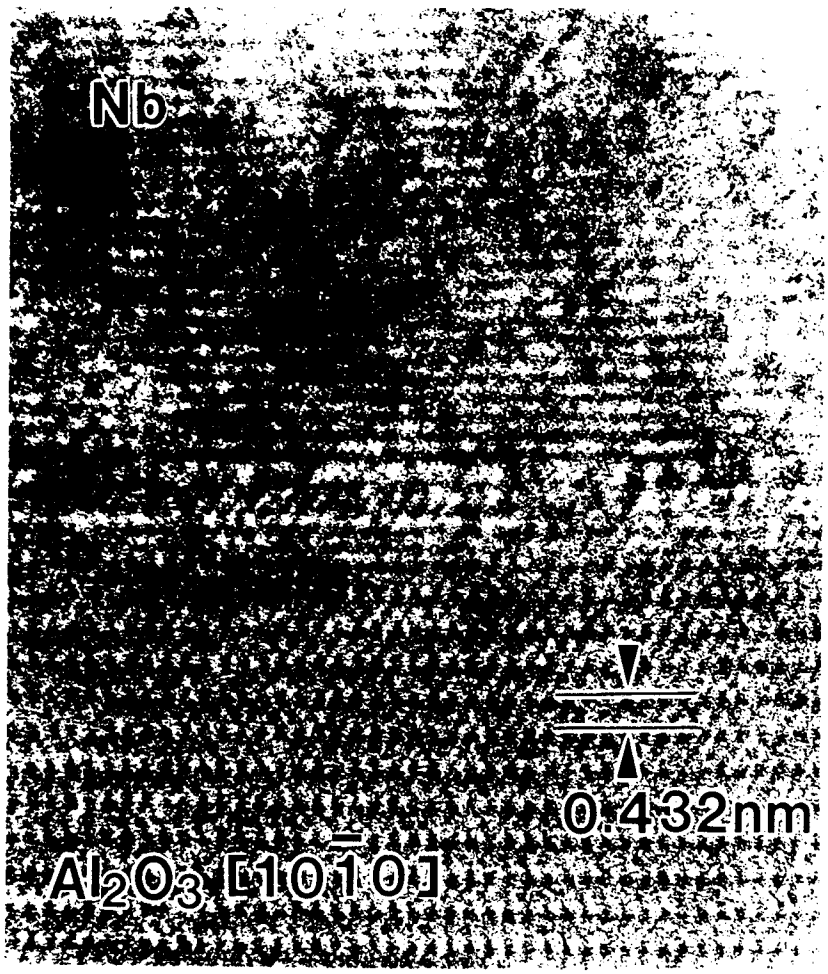


Figure 6.

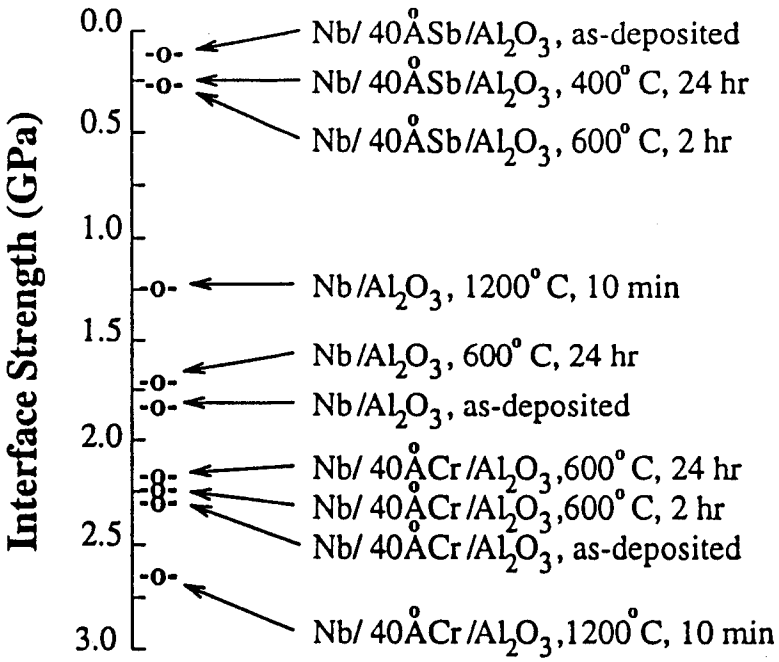


Figure 7a. Interface strengths as measured by the modified laser spallation experiment.

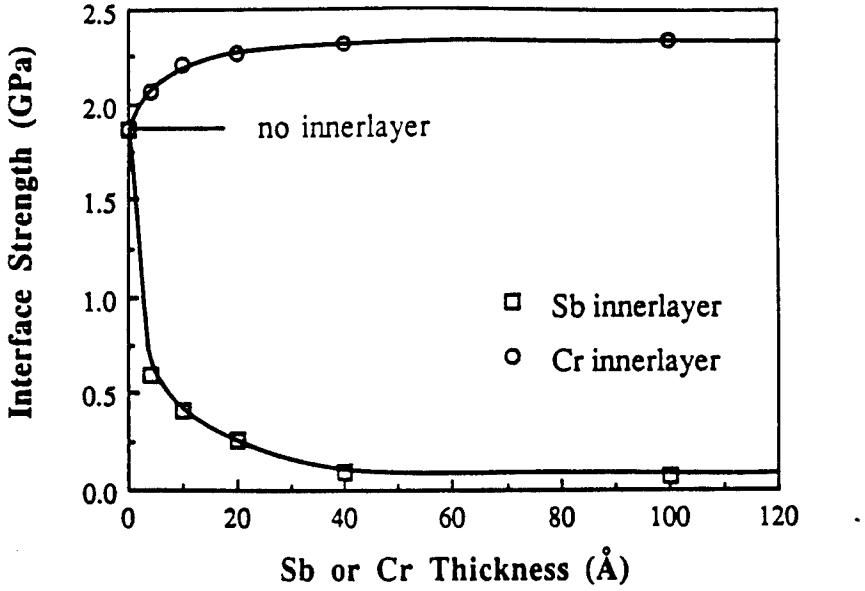


Figure 7b. The control of Nb/sapphire interface strength through control of Cr and Sb interlayer thickness.

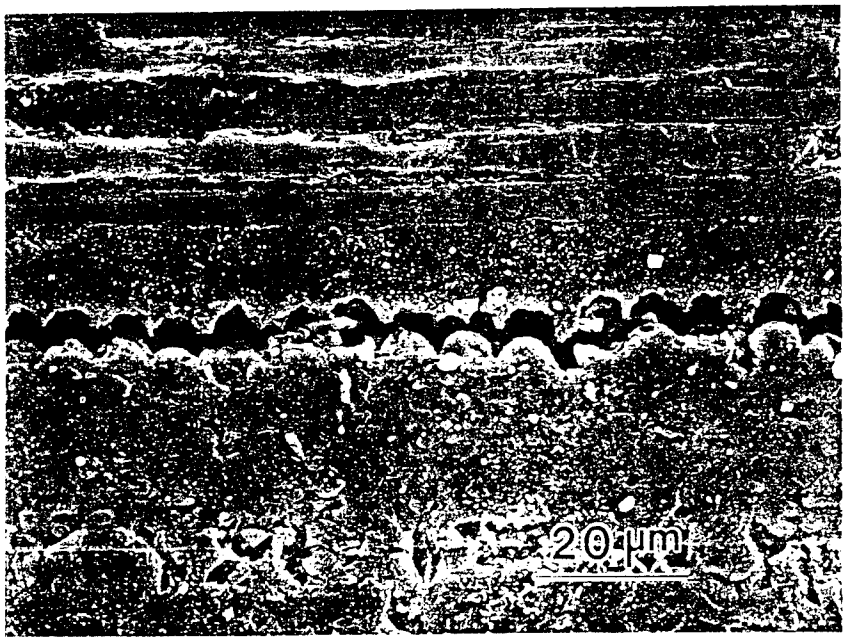


Figure 8 : A high magnification view of the intra bundle crack in the C/P sample showing the local failure to be through the matrix and the fiber matrix interface.

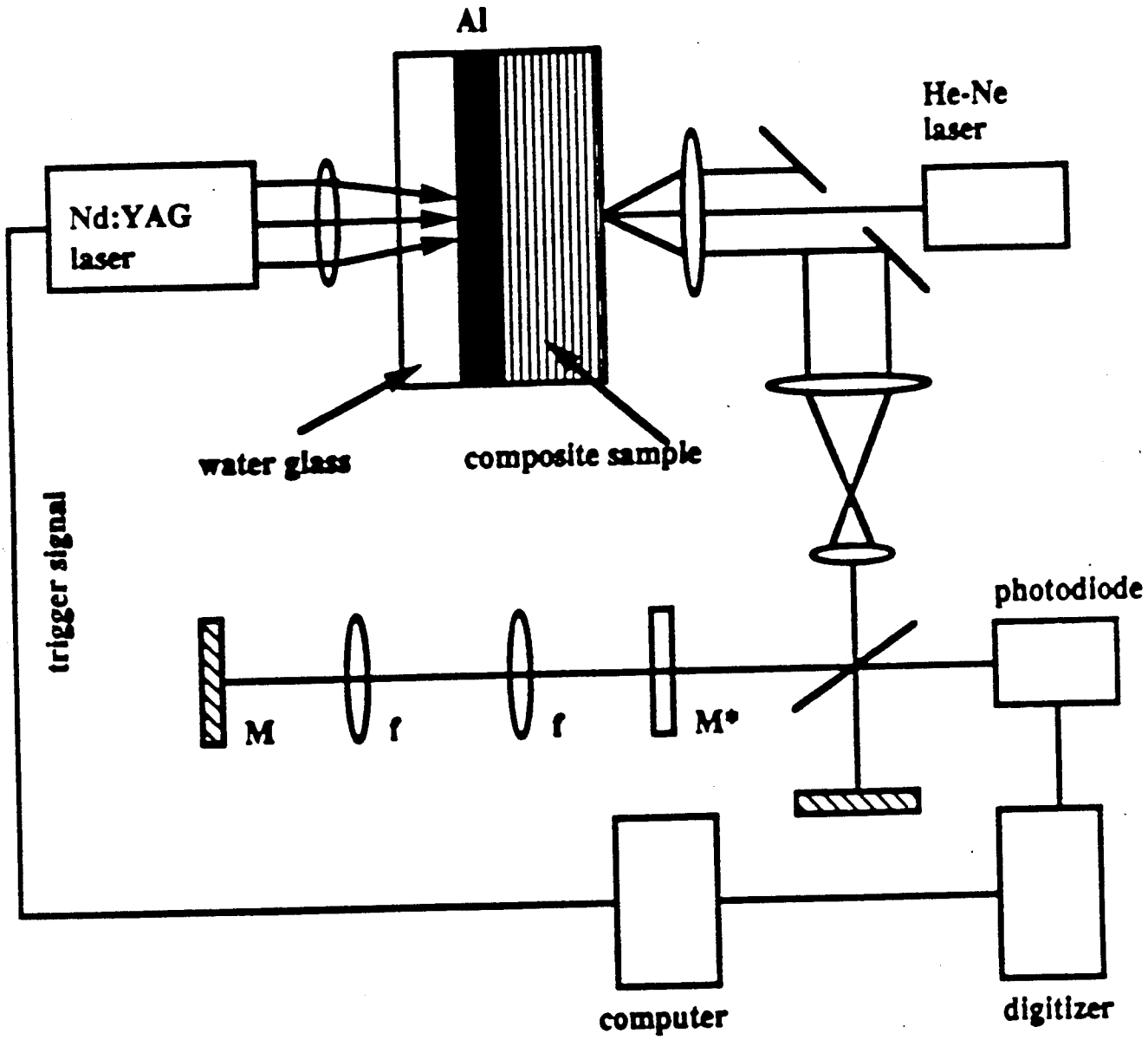


Figure 9 . Schematic of the spallation experiment along with the modified laser Doppler interferometer for diffuse surfaces.

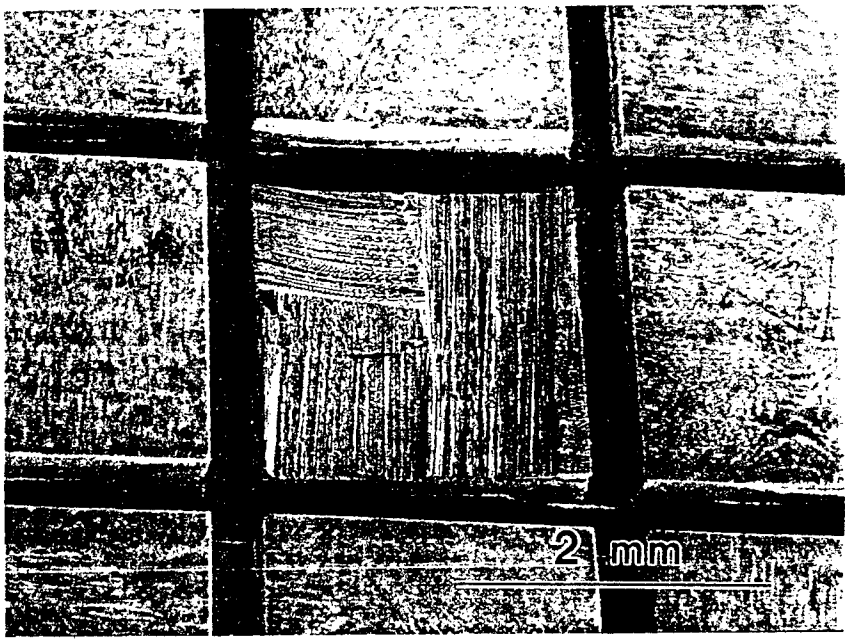


Figure 10: A micrograph showing spallation in a central square coupon when the stress pulse was generated on the back surface and in line with the central coupon. The failure was at the interply interface since no tearing of the fibers within the bundles was observed on the two separated surfaces. The above micrograph is for the C/P laminate. Almost identical failure results in the C/C samples with the same square coupon geometry and groove depths.

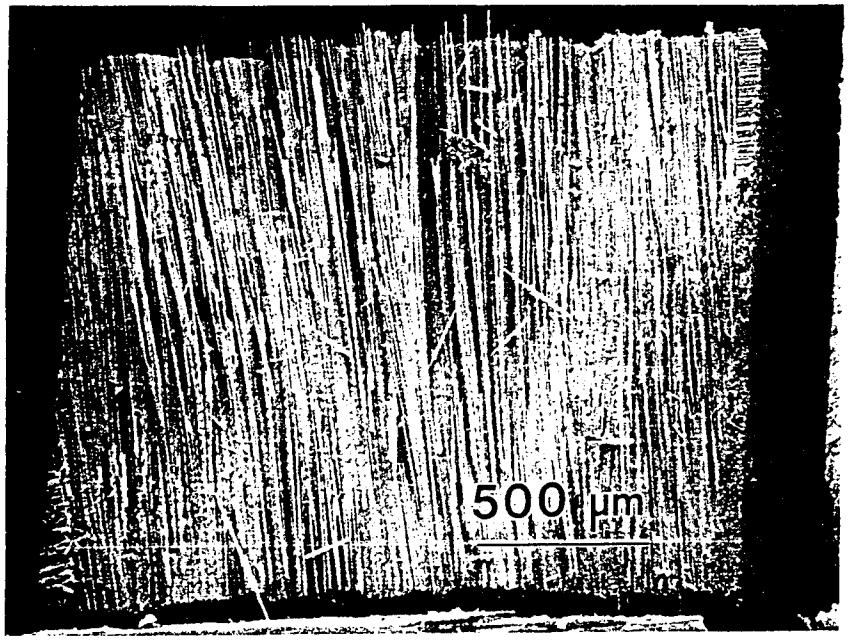


Figure 1: A micrograph showing the spallation within parallel fiber bundles as indicated by the similarly oriented fibers on the fractured surface.

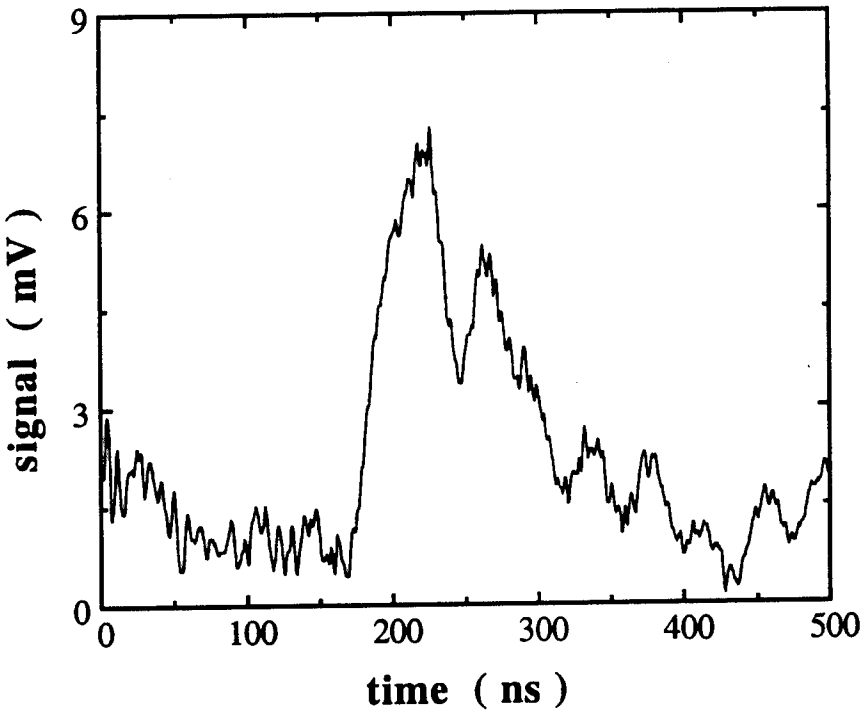


Figure 8: The velocity profile measured at the free surface of a 0.55 mm thick C/P sample.

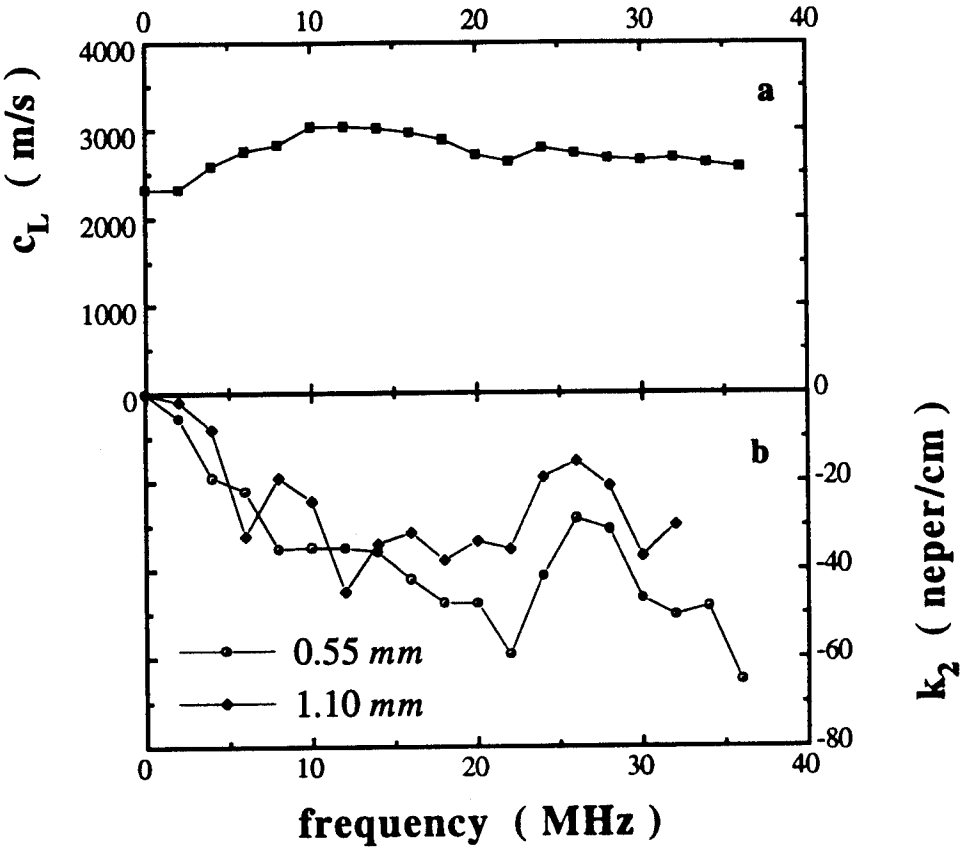


Figure 13 Data showing the dispersion characteristics for the C/P laminate with local microstructure given in Fig. 3(b). The imaginary part of the wave number $k$ gives the velocity of the dilatational wave, presented as a function of frequency in (a). The attenuation for different frequencies in the C/P microstructure is shown in (b).

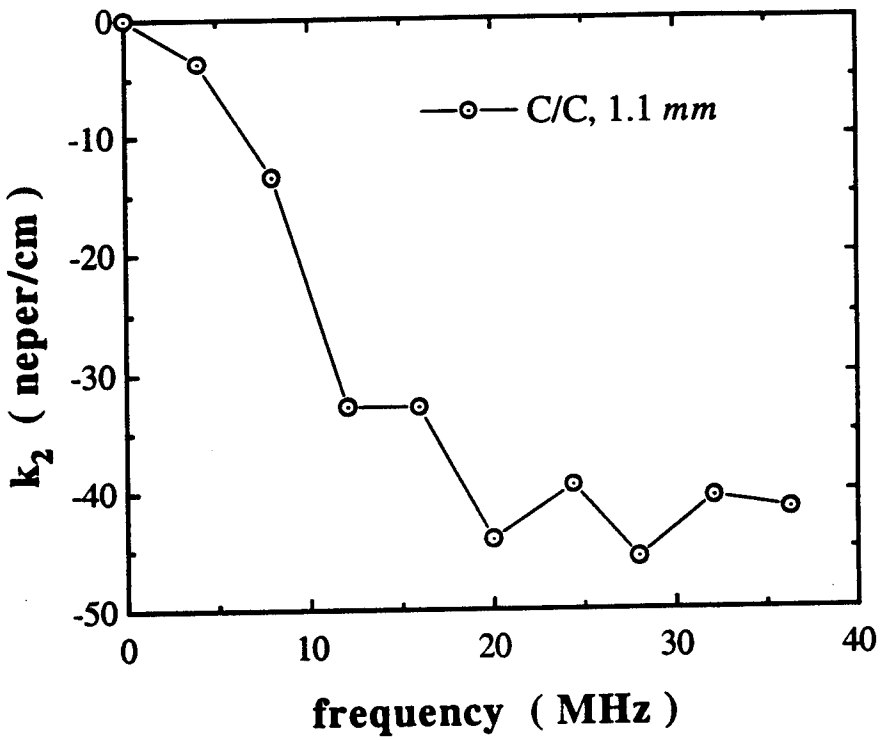


Figure 14 Data showing the attenuation of different frequencies for the C/C microstructure given in Fig. 3(a).

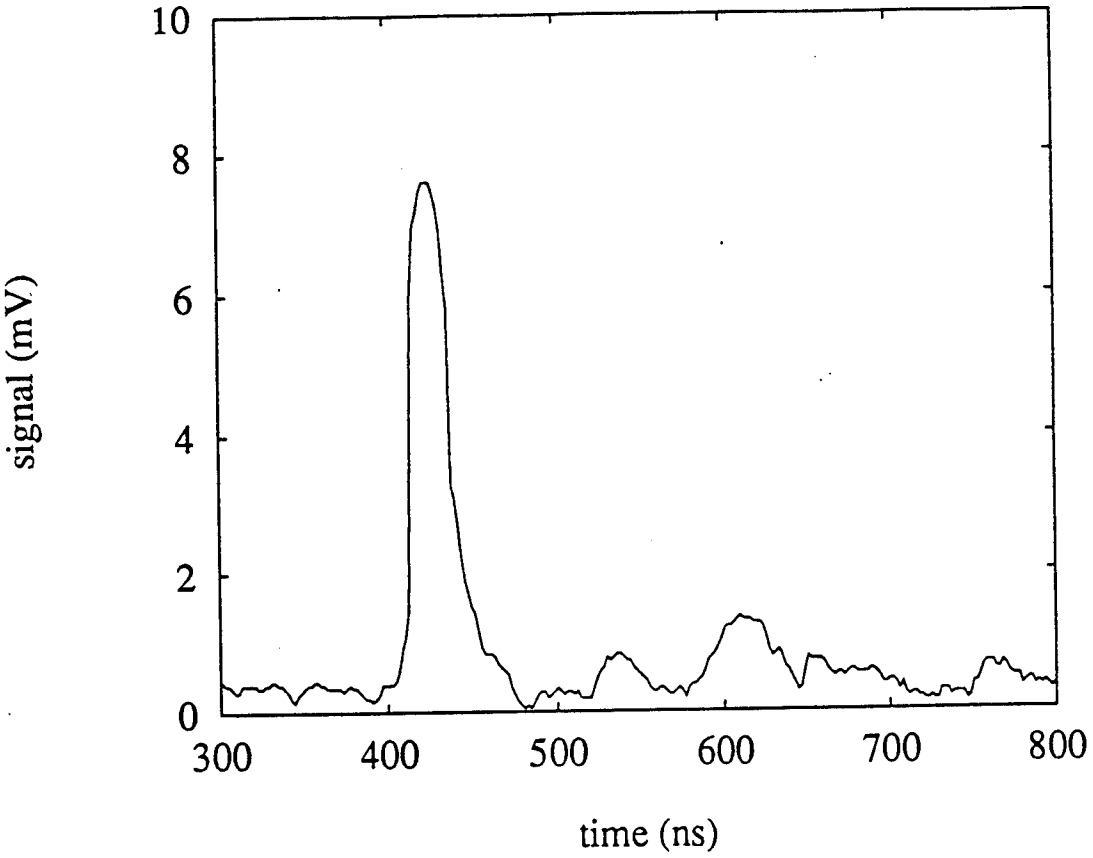


Figure 15.

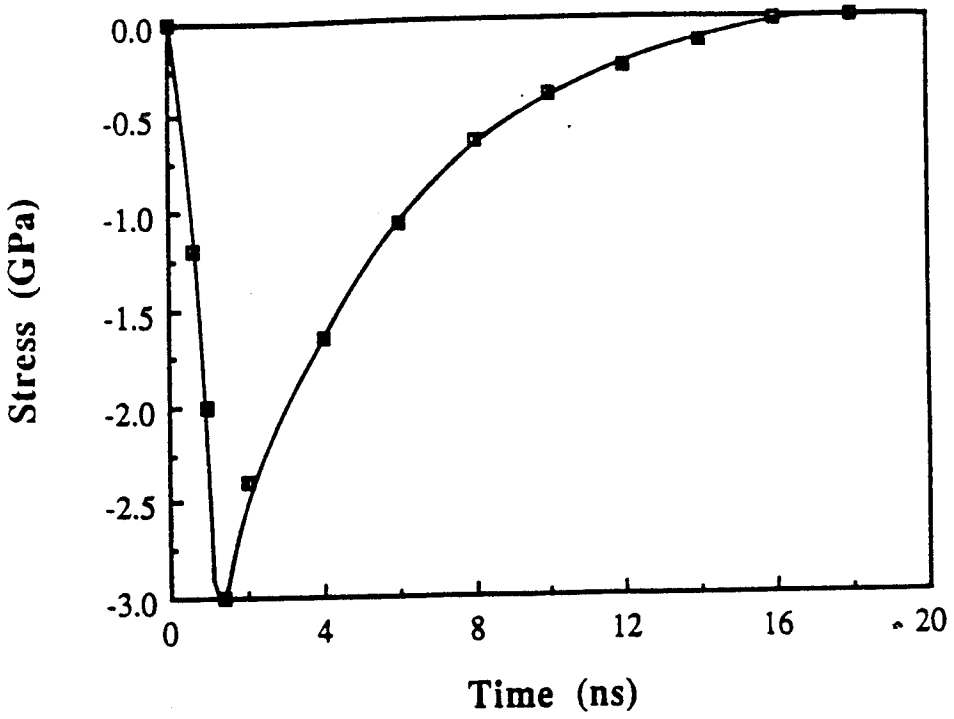


Figure 16 The stress pulse profile generated at the laser fluence of $8.67 \times 10^5$ J/m$^2$.

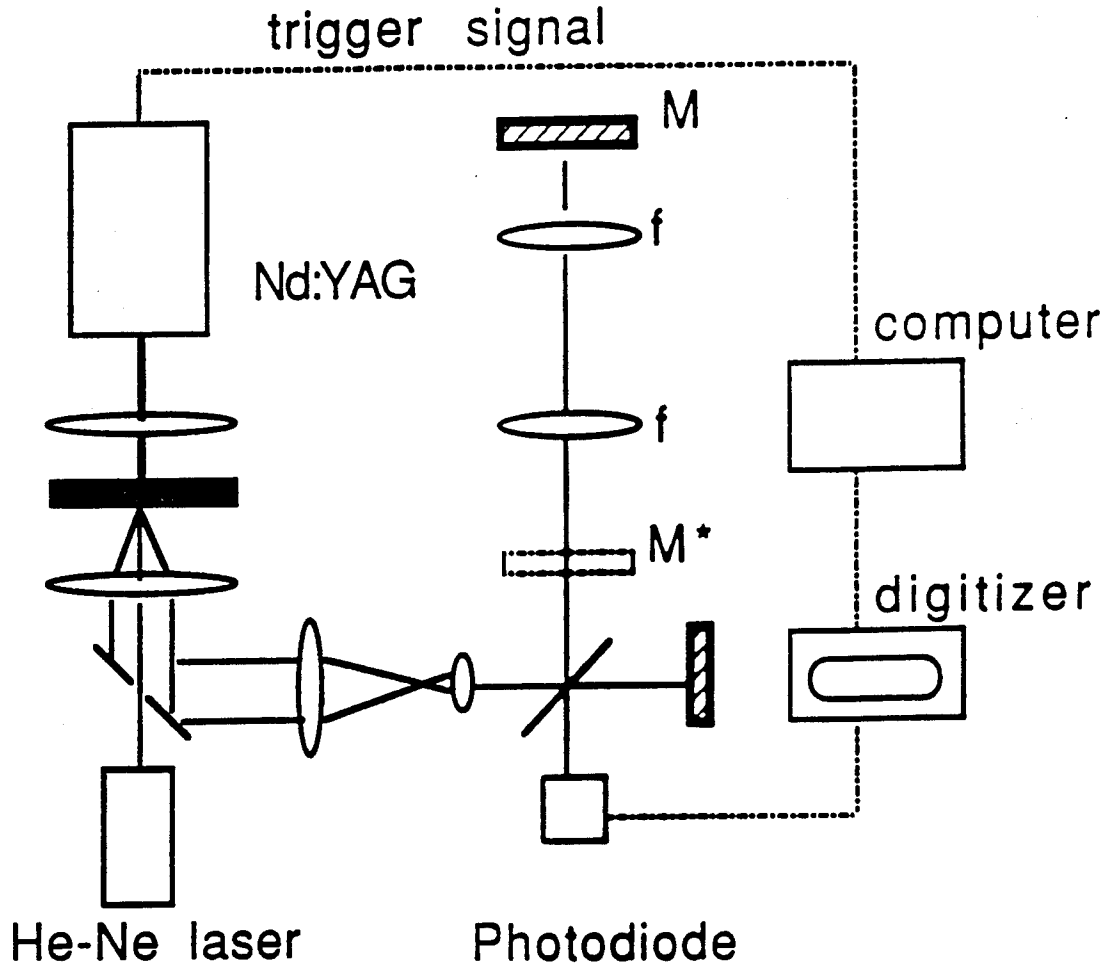


Figure 17